



### Unexpected reactivity of a PONNOP 'expanded pincer' ligand†

Arthur R. Scheerder,<sup>a</sup> Martin Lutz<sup>b</sup> and Daniël L. J. Broere<sup>id</sup>\*<sup>a</sup>

Cite this: *Chem. Commun.*, 2020, 56, 8198

Received 24th March 2020,  
Accepted 29th April 2020

DOI: 10.1039/d0cc02166k

rsc.li/chemcomm

**We report the synthesis, characterization and coordination chemistry of a new naphthyridine-derived phosphinite PONNOP expanded pincer ligand. As envisioned, the dinucleating ligand readily binds two copper(i) centers in close proximity, but undergoes an unexpected rearrangement in the presence of nickel(ii) salts to form an interesting PONNP pincer platform.**

The use of well-defined bimetallic complexes wherein two metal atoms are bound in close proximity is an emerging area in homogeneous catalysis.<sup>1</sup> The cooperative activation of substrate molecules by two metal centers in such bimetallic systems can enable distinct reactivity or improved catalytic performance when compared to monometallic analogues.<sup>2</sup> The design and exploration of new dinucleating ligands that enable such metal–metal cooperativity is key to further explore the potential of bimetallic catalysis. A motif well-suited to bind two metals is the 1,8-naphthyridine scaffold.<sup>3</sup> Yet, relatively few ligands derived thereof have been reported that are capable of both binding two metal centers in close proximity while also providing accessible adjacent coordination sites on both metals to enable metal–metal cooperativity.<sup>4</sup> In the pursuit of such new platforms we recently reported a dinucleating 'expanded PNNP' pincer ligand,<sup>5</sup> which was inspired by the mononucleating PNP pincer ligands<sup>6</sup> (Scheme 1, top). Similar to the PNP ligands the CH<sub>2</sub> linkers in the PNNP ligand can be deprotonated concomitant with dearomatization of the naphthyridine core, and this enabled the cooperative activation of H<sub>2</sub> to give a tetranuclear copper dihydride cluster.<sup>7</sup>

Exchanging the acidic CH<sub>2</sub> linkers in the PNP pincer ligands by O atoms affords the diphosphinite PONNOP pincer ligand (Scheme 1, bottom), which was developed independently by the Milstein<sup>8</sup> and Goldberg & Brookhart<sup>9</sup> groups. The PONNOP pincer ligand has been utilized to stabilize various metal complexes and, for example, has enabled the detailed study of dihydrogen complexes of Rh and Ir,<sup>10</sup>  $\sigma$ -alkane complexes,<sup>11</sup> and more recently photolytic N<sub>2</sub> reduction to NH<sub>3</sub> using Re.<sup>12</sup> Given the distinct differences between the PNP and PONNOP pincer ligands we were interested to study a PNNP analogue wherein the reactive methylene linkers are replaced by oxygen atoms. Herein, we describe the synthesis, characterization and coordination chemistry of a new expanded pincer ligand, <sup>i</sup>Pr-PONNOP. Similar to the PNNP analogue, <sup>i</sup>Pr-PONNOP can bind two copper atoms in close proximity. However, we found that this ligand undergoes an unusual rearrangement in the presence of nickel salts. Although this rearrangement provides access to a unique 'regular' pincer ligand, it

Deprotonation of acidic CH<sub>2</sub> results in dearomatization



Different electronic properties and no acidic protons



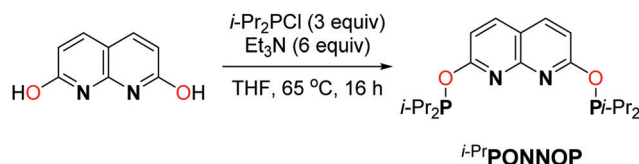
<sup>a</sup> *Organic Chemistry and Catalysis, Debye Institute for Nanomaterials Science Faculty of Science, Utrecht University, Universiteitsweg 99, 3584 CG, Utrecht, The Netherlands. E-mail: d.l.j.broere@uu.nl*

<sup>b</sup> *Crystal and Structural Chemistry, Bijvoet Centre for Biomolecular Research Faculty of Science, Utrecht University, Padualaan 8, 3584 CH Utrecht, The Netherlands*

† Electronic supplementary information (ESI) available: NMR, IR and X-ray crystallographic data and synthetic procedures for all compounds. CCDC 1990856–1990858. For ESI and crystallographic data in CIF or other electronic format see DOI: 10.1039/d0cc02166k

Scheme 1 Comparison of the PNP and PONNOP pincer ligands with the PNNP and PONNOP expanded pincer ligands.



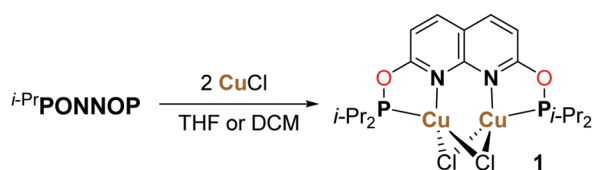


Scheme 2 The synthesis of the  $i\text{-PrPONNOP}$  "expanded pincer" ligand.

can prohibit binding two metal centers in close proximity, and should therefore be taken into consideration in the design of naphthyridine-derived dinucleating ligands featuring phosphinite donors.<sup>13</sup>

The phosphinite expanded pincer ligand  $i\text{-PrPONNOP}$  was prepared in a three-step procedure from commercially available starting materials in an overall yield of 37%. The first two steps comprise the synthesis of 2,7-dihydroxy-1,8-naphthyridine according to a modified literature procedure.<sup>14</sup> Subsequent phosphorylation was achieved by a reaction with a slight excess of chlorodiisopropylphosphine in the presence of excess  $\text{Et}_3\text{N}$  in THF at 65 °C (Scheme 2) affording  $i\text{-PrPONNOP}$  as a brown oil in 82% yield and 90% purity after workup. Several attempts to further enhance the purity solely resulted further decrease in purity due to the facile hydrolysis of the P–O bonds in the expanded pincer ligand (see ESI† for more detail). The related 2,6-dihydroxypyridine-derived  $i\text{-PrPONOP}$  pincer ligand was also reported in 90% purity.<sup>8</sup> Fortunately, the unidentified impurities in the expanded pincer ligand are readily removed in subsequent reactions (see below). The  $^1\text{H}$ ,  $^{13}\text{C}$  and  $^{31}\text{P}$  NMR spectra of  $i\text{-PrPONNOP}$  in  $\text{C}_6\text{D}_6$  at 298 K show the expected number of resonances for a  $C_{2v}$  symmetric species. The  $^{31}\text{P}\{^1\text{H}\}$  NMR spectrum shows a singlet at  $\delta = 148.2$  ppm, similar to the observed resonance for the  $i\text{-PrPONOP}$  pincer ( $\delta = 149.1$  ppm).<sup>8</sup>

Reacting  $i\text{-PrPONNOP}$  with 2 equiv. of  $\text{CuCl}$  in THF or  $\text{CH}_2\text{Cl}_2$  (Scheme 3) gives the dicopper(I) complex **1**, which was isolated as yellow-orange powder in 77% yield. The  $^1\text{H}$ ,  $^{13}\text{C}$  and  $^{31}\text{P}$  NMR spectra of **1** in  $\text{CD}_2\text{Cl}_2$  show that the  $C_{2v}$  symmetry is retained upon binding the Cu centers. The  $^{31}\text{P}$  NMR spectrum of **1** in  $\text{CD}_2\text{Cl}_2$  features a single broad resonance at  $\delta = 123.7$  ppm. VT NMR analysis (Fig. S14–S19, ESI†) showed that the broadness is not due to a fluxional process on the NMR time scale. This suggests that it originates from quadrupolar relaxation arising from  $^{63}\text{Cu}$  and  $^{65}\text{Cu}$  (both  $I = 3/2$ ) nuclei, which is not uncommon for Cu(I) phosphinite complexes.<sup>15</sup> Crystals suitable for single-crystal X-ray diffraction were grown by vapor diffusion of hexane into a THF solution of **1** at ambient temperature. The solid-state structure of **1** (Fig. 1) revealed a nearly flat dinucleating phosphinite ligand bound to a diamond-shaped  $\text{Cu}_2\text{Cl}_2$  core. The structure is similar to the previously reported



Scheme 3 Synthesis of the dicopper(I) complex **1**.

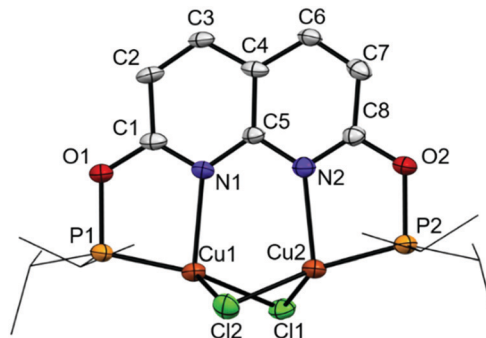


Fig. 1 Displacement ellipsoid plot (50% probability) of complex **1** in the crystal. Hydrogen atoms and THF solvent molecule are omitted, and  $i\text{-Pr}$  groups on P are depicted as wireframe for clarity.

$i\text{-BuPNNPCu}_2\text{Cl}_2$ <sup>7</sup> but features a Cu–Cu distance (2.7224(9) Å) that is  $\sim 0.14$  Å longer, and PN bite angles ( $\angle \text{P1–Cu1–N1} = 83.33(14)^\circ$  and  $\angle \text{P2–Cu2–N2} = 83.00(14)^\circ$ ) that are smaller by  $\sim 3^\circ$  (see Tables S3–S5, ESI† for more detail).

As the P–O bonds in the phosphinite expanded pincer ligand are highly susceptible to hydrolysis, the use of solvents containing trace water typically results in precipitation of 2,7-dihydroxy-1,8-naphthyridine and the formation of a partial hydrolysis product  $i\text{-PrPONNOH}$ . The latter monophosphinite displays four characteristic aromatic resonances in  $^1\text{H}$  NMR spectra of reaction mixtures and is also observed as an intermediate in the synthesis of  $i\text{-PrPONNOP}$  (see ESI† for more detail). Both these undesired naphthyridine containing products were also observed in several reactions as a result of alcoholysis or aminolysis. For example, a reaction in THF of  $i\text{-PrPONNOP}$  with 2 equiv.  $\text{NiCl}_2$  containing residual EtOH resulted in the formation of an insoluble 2,7-dihydroxy-1,8-naphthyridine-derived species and  $\text{trans-NiCl}_2(\text{P}(\text{OEt})(i\text{-Pr})_2)_2$ , which was isolated and crystallographically characterized (see ESI† for more detail). Nonetheless, when using rigorously dried solvents these undesired side reactions can be prevented.

Reacting  $i\text{-PrPONNOP}$  with 2 equiv.  $\text{NiBr}_2$  in THF results in the formation of an insoluble precipitate and a single species in solution that features four aromatic resonances in the  $^1\text{H}$  NMR spectrum, indicative of a loss of  $C_{2v}$  symmetry. Unlike the partial hydrolysis product  $i\text{-PrPONNOH}$ , this unsymmetrical species contains two diisopropylphosphinite moieties, which appear as two doublets ( $^2J_{\text{PP}} = 326$  Hz) at  $\delta = 192.0$  and 131.5 ppm in the  $^{31}\text{P}$  NMR spectrum in  $\text{CD}_2\text{Cl}_2$ . To our surprise single-crystal X-ray structure determination (Fig. 2) did not reveal a dinuclear complex but showed mononuclear complex **2**, which is consistent with the  $^1\text{H}$ ,  $^{13}\text{C}$  and  $^{31}\text{P}$  NMR spectra as well as the CHN elemental analysis of the obtained solid. Furthermore, complex **2** can also be prepared in 89% yield by a reaction of  $i\text{-PrPONNOP}$  ligand with 1 equiv.  $\text{NiBr}_2$  in  $\text{CH}_2\text{Cl}_2$  (Scheme 4). The solid state structure (Fig. 2) shows that the expanded pincer ligand underwent a rearrangement to form an interesting naphthyridone-like  $i\text{-PrPONNP}$  "regular" pincer ligand bound to nickel. The nickel atom exhibits a slightly distorted square pyramidal geometry with a Br atom in the apical position. Nickel(II) pentacoordination is uncommon in pincer chemistry<sup>16</sup> and all reported  $\text{NiX}_2$  ( $\text{X} = \text{Cl}$  or  $\text{Br}$ )



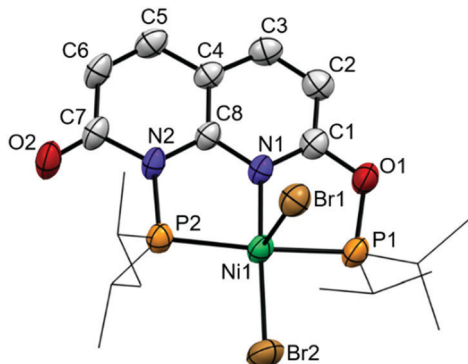
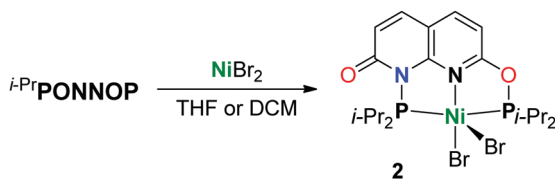


Fig. 2 Displacement ellipsoid plot (50% probability) of complex **2** in the crystal. Hydrogen atoms and THF solvent molecules are omitted, and *i*-Pr groups on P are depicted as wireframe for clarity.



Scheme 4 Synthesis of the mononuclear Ni complex **2**.

complexes bearing related lutidine-derived PNP,<sup>17–19</sup> PONOP<sup>20</sup> and PNNP<sup>21</sup> pincer ligands display square planar geometries with a non-coordinated halide anion. The nickel bromide bond lengths in **2** differ greatly, and the distance is significantly longer for the bromide in the apical position (Ni1–Br1 = 2.7852(8) Å) than what is observed for the bromide in the basal position (Ni1–Br2 = 2.3200(8) Å). A similar observation was made for a dibromo{bis[2-(diphenylphosphanyl)ethyl]amine} Ni(II) complex, which showed an apical Ni–Br bond of 2.698(7) Å and a basal Ni–Br bond of 2.333(7) Å.<sup>22</sup> A rare example of a related penta-coordinated Ni(PNNP) pincer complex with an anionic phosphinite instead of a basal Br ligand, showed an significantly shorter apical Ni–Br bond of 2.535(4) Å.<sup>23</sup> The intraligand bond metrics are distinctly different from those in complex **1** (Table S6, ESI†). The C7–O2 bond length of 1.214(6) Å is significantly shorter than the C1–O1 bond length of 1.346(5) Å. This observation indicates a dearomatization of the six-membered heterocycle containing N2 to form a localized naphthyridone, and this is further underlined by the clear localization of single and double bonds in this ring (Fig. S29, ESI†). We reason that the rearrangement of the *i*-Pr-PONNOP ligand to the pincer ligand present in complex **2** is also enabled by the ability to form a naphthyridone structure.

To gain insight into why the ligand rearrangement is only observed with NiBr<sub>2</sub> and not with CuCl we studied the interconversion of the PONNOP and PONNP isomers computationally. Both isomers and the transition state geometries for their conversion were optimized (BP86-D3, def2-TZVP) without a metal, bound to CuCl or bound to NiBr<sub>2</sub> (see ESI† for more details and discussion). Unfortunately, the heterogeneous nature of the studied reactions and the high sensitivity of the *i*-Pr-PONNOP ligand

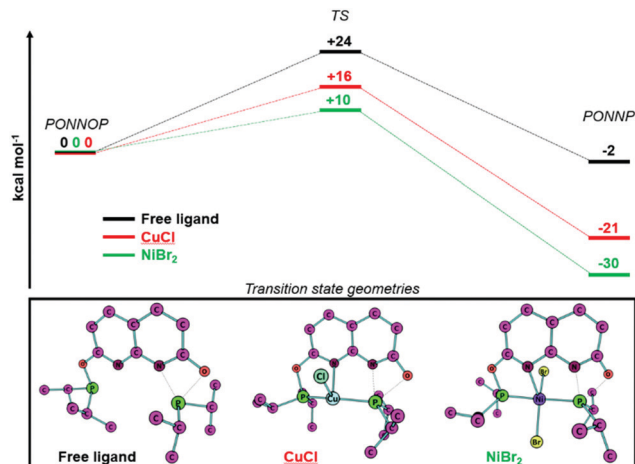


Fig. 3 DFT calculated (BP86-D3, def2-TZVP) free energy profiles ( $\Delta G_{298K}^{\ddagger}$  in kcal mol<sup>-1</sup>) for the rearrangement of PONNOP to PONNP (top) and the transition state geometries (bottom).

prohibited experimental validation of the computational methods beyond a good agreement of the experimental and computational geometries of complex **2**. Hence, we refrain from putting much value on the absolute energies and choose to only look at the general trends, which provide some insight. The calculated free energy profile for the free ligand (Fig. 3, top) shows that the PONNOP and PONNP isomers are similar in energy and that there is a relatively high barrier for their interconversion. Heating a toluene solution of *i*-Pr-PONNOP for multiple hours at 110 °C showed no conversion into a new species based on NMR analysis indicating that either the barrier for the interconversion is too high or that the PONNOP isomer is the thermodynamic product.<sup>24</sup> Notably, when the PONNOP ligand is bound to either CuCl or NiBr<sub>2</sub> the calculated free energies of the PONNP isomer are significantly more stable than the PONNOP isomer. Similarly, the calculated energy barrier for the conversion of the PONNOP isomer to the PONNP is also significantly lower. Upon analysis of the corresponding transition state geometries (Fig. 3, bottom) it can be seen that the P atom, which migrates from O to N is bound to the transition metal atom. Although this also results in significant bending of the naphthyridine core (Fig. S33, ESI†), we reason that this provides the additional stabilization of the transition state to enable the isomerization towards the more stable PONNP pincer motif. We hypothesize that these effects are most pronounced when the ligand is bound to NiBr<sub>2</sub> because the TS and PONNP geometries are closer to the preferred coordination geometry of Ni(II) than of that of Cu(I) (see ESI† for more detail). Although dinuclear complex **1** was obtained in high yield, we reacted *i*-Pr-PONNOP with one equiv. of CuCl since the calculated free energy profile indicated facile formation of a PONNP pincer complex of CuCl. Unfortunately, no conclusions can be drawn from this experiment as it resulted in the formation of an inseparable mixture of unidentified unsymmetrical species. The broadness of the resonances due to coordination to Cu also obscured the observation of a potential characteristic *trans* coupling like that observed in the <sup>31</sup>P NMR spectrum of **2**. We reason that the facile formation of **2** is likely fast and irreversible under



the experimental conditions, and this is in agreement with the calculated free energy profile that features a low barrier and is very exergonic. In contrast, it is conceivable that with Cu the binding of a second CuCl is associated with a lower energy barrier, and therefore kinetically favored over the rearrangement. An alternative explanation is that the rearrangement is reversible in the presence of excess CuCl, and perhaps mediated by binding to a second Cu center. Unfortunately, since various attempts at reactions of  $i^{\text{-Pr}}\text{PONNOP}$  with 1 equiv. CuCl or 2 equiv. NiBr<sub>2</sub> did not give a monocopper or dinickel species, respectively, we have thus far been unable to verify these hypotheses.

In conclusion, we have described the synthesis, characterization and coordination chemistry of a new diphosphinite expanded pincer ligand,  $i^{\text{-Pr}}\text{PONNOP}$ . This new dinucleating ligand does not feature the acidic methylene linkers that are present in the related PNNP ligand, and binds two copper centers in close proximity in a similar fashion. In contrast, attempts to bind two nickel centers resulted in a ligand rearrangement concomitant with the formation of a unique naphthyridone PONNP pincer ligand. This work adds a new, readily synthesized dinucleating ligand to the bimetallic catalysis toolkit. Moreover, the results herein demonstrate that naphthyridine-derived ligands featuring phosphinite donors should be used with caution as they are able to undergo a rearrangement under certain conditions to form a 'regular' pincer ligand. Although the latter is undesired for bimetallic chemistry, it does provide access to an otherwise inaccessible ligand class for mononuclear chemistry.

This work was supported by Utrecht University (tenure track start-up package to D. L. J. B.), The Netherlands Organization for Scientific Research (START-UP grant 740.018.019 to D. L. J. B.) and the European Union's Horizon 2020 research and innovation program (agreement 840836, MSCA-IF to D. L. J. B., BiMetaCat). Access to supercomputer facilities was sponsored by NWO Exacte en Natuurwetenschappen (Physical Sciences). The X-ray diffractometer was financed by the NWO. Lada Dabranskaya is acknowledged for her artistic input for the TOC graphic. NMR and ORCA data files can be obtained free of charge from: <http://doi.org/10.4121/uuid:8fd78884-01b0-4c37-a4ca-fb1cf4af8b61>.

## Conflicts of interest

There are no conflicts to declare.

## Notes and references

- (a) N. Xiong, G. Zhang, X. Sun and R. Zeng, *Chin. J. Chem.*, 2020, **38**, 185–201; (b) R. B. Ferreira and L. J. Murray, *Acc. Chem. Res.*, 2019, **52**, 447–455; (c) S. Rej, H. Tsurugi and K. Mashima, *Coord. Chem. Rev.*, 2018, **355**, 223–239; (d) I. G. Powers and C. Uyeda, *ACS Catal.*, 2017, **7**, 936–958; (e) D. R. Pye and N. P. Mankad, *Chem. Sci.*, 2017, **8**, 1705–1717; (f) N. P. Mankad, *Chem. – Eur. J.*, 2016, **22**, 5822–5829; (g) M. Iglesias, E. Sola and L. A. Oro, in *Homo and Heterobimetallic Complexes in Catalysis: Cooperative Catalysis*, ed. P. Kalck, Springer International Publishing, Cham, 2016, pp. 31–58.
- Selected recent examples: (a) H.-C. Yu, S. M. Islam and N. P. Mankad, *ACS Catal.*, 2020, **10**, 3670–3675; (b) Y.-Y. Zhou and C. Uyeda, *Science*, 2019, **363**, 857–862; (c) K. M. Gramigna, D. A. Dickie, B. M. Foxman and C. M. Thomas, *ACS Catal.*, 2019, **9**, 3153–3164; (d) I. G. Powers, J. M. Andjaba, X. Luo, J. Mei and C. Uyeda, *J. Am. Chem. Soc.*, 2018, **140**, 4110–4118.
- J. K. Bera, N. Sadhukhanb and M. Majumdar, *Eur. J. Inorg. Chem.*, 2009, 4023–4038.
- Selected examples of ligand platforms: (a) M. S. Ziegler, D. S. Levine, K. V. Lakshmi and T. D. Tilley, *J. Am. Chem. Soc.*, 2016, **138**, 6484–6491; (b) T.-T. Zhou, D. R. Hartline, T. J. Steiman, P. E. Fanwick and C. Uyeda, *Inorg. Chem.*, 2014, **53**, 11770–11777; (c) E. Binamira-Soriaga, N. L. Keder and W. C. Kaska, *Inorg. Chem.*, 1990, **29**, 3167–3171; (d) T.-P. Cheng, B.-S. Liao, Y.-H. Liu, S.-M. Penga and S.-T. Liu, *Dalton Trans.*, 2012, **41**, 3468–3473; (e) C. He, A. M. Barrios, D. Lee, J. Kuzelka, R. M. Davydov and S. J. Lippard, *J. Am. Chem. Soc.*, 2000, **122**, 12683–12690; (f) A. Nicolay and T. D. Tilley, *Chem. – Eur. J.*, 2018, **24**, 10329–10333.
- E. Kounalis, M. Lutz and D. L. J. Broere, *Organometallics*, 2020, **39**, 585–592.
- (a) *Organometallic Pincer Chemistry*, ed. G. van Koten and D. Milstein, Springer, Berlin, 2013, vol. 40; (b) *The Privileged Pincer-Metal Platform: Coordination Chemistry & Applications Top Organometallic Chem*, ed. G. van Koten and R. A. Gossage, Springer, 2016, vol. 54; (c) *Pincer and Pincer-Type Complexes: Applications in Organic Synthesis and Catalysis*, ed. K. J. Szabó and O. Wendt, Wiley, 2014.
- E. Kounalis, M. Lutz and D. L. J. Broere, *Chem. – Eur. J.*, 2019, **25**, 13280–13284.
- H. Salem, L. J. W. Shimon, Y. Diskin-Posner, G. Leitus, Y. Ben-David and D. Milstein, *Organometallics*, 2009, **28**, 4791–4806.
- W. H. Bernskoetter, S. Kloek Hanson, S. K. Buzak, Z. Davis, P. S. White, R. Swartz, K. I. Goldberg and M. Brookhart, *J. Am. Chem. Soc.*, 2009, **131**, 8603–8613.
- M. Findlater, K. M. Schultz, W. H. Bernskoetter, A. Cartwright-Sykes, D. M. Heinekey and M. Brookhart, *Inorg. Chem.*, 2012, **51**, 4672–4678.
- (a) M. D. Walter, P. S. White, C. K. Schauer and M. Brookhart, *J. Am. Chem. Soc.*, 2013, **135**, 15933–15947; (b) J. Campos, S. Kundu, D. R. Pahls, M. Brookhart, E. Carmona and T. R. Cundari, *J. Am. Chem. Soc.*, 2013, **135**, 1217–1220.
- Q. J. Bruch, G. P. Connor, C.-H. Chen, P. L. Holland, J. M. Mayer, F. Hasanayn and A. J. M. Miller, *J. Am. Chem. Soc.*, 2019, **141**, 20198–20208.
- While this manuscript was in preparation an interesting ligand system for the selective synthesis of heterobimetallic complexes that features such a naphthyridine-derived phosphinite system was reported: S. Deolka, O. Rivada Wheelaghan, S. Aristizábal, R. Fayzullin, S. Pal, K. Nozaki, E. Khaskin and J. Khusnutdinova (2020): Metal–Metal Cooperative Bond Activation by Heterobimetallic Alkyl, Aryl, and Acetylide PtII/CuI Complexes. ChemRxiv. Preprint. <https://doi.org/10.26434/chemrxiv.11742687.v1>.
- P. S. Lempert, P. N. Ostapchuk, A. A. Bobrikova, P. V. Petrovskii, N. D. Kagramanov, G. V. Bodrin and E. E. Nifant'ev, *Mendeleev Commun.*, 2010, **20**, 223–225.
- A. Marker and M. J. Gunter, *J. Magn. Reson.*, 1982, **47**, 118–132.
- D. M. Roddick and D. Zargarian, *Inorg. Chim. Acta*, 2014, **422**, 251–264.
- Z. Yang, D. Liu, Y. Liu, M. Sugiya, T. Imamoto and W. Zhang, *Organometallics*, 2015, **34**, 1228–1237.
- M. Vogt, O. Rivada-Wheelaghan, M. A. Iron, G. Leitus, Y. Diskin-Posner, L. J. W. Shimon, Y. Ben-David and D. Milstein, *Organometallics*, 2013, **32**, 300–308.
- S. Lapointe, E. Khaskin, R. R. Fayzullin and J. R. Khusnutdinova, *Organometallics*, 2019, **38**, 1581–1594.
- S. Kundu, W. W. Brennessel and W. D. Jones, *Inorg. Chem.*, 2011, **50**, 9443–9453.
- D. Benito-Garagorri, E. Becker, J. Wiedermann, W. Lackner, M. Pollak, K. Mereiter, J. Kisala and K. Kirchner, *Organometallics*, 2006, **25**, 1900–1913.
- P. L. Orioli and C. A. Ghilardi, *J. Chem. Soc. A*, 1970, 1511–1516.
- D. Benito-Garagorri, K. Mereiter and K. Kirchner, *Eur. J. Inorg. Chem.*, 2006, 4374–4379.
- Although the computations suggest that the PONNP isomer is the thermodynamic product (by only 2 kcal mol<sup>-1</sup>), we consider this subtle difference to be within the uncertainty of our non-benchmarked DFT method.

